Polymer Testing 57 (2017) 119–125

Contents lists available at ScienceDirect

Polymer Testing

journal homepage: www.elsevier.com/locate/polytest

Material Behaviour

Thermal-mechanical behavior of styrene-based shape memory polymer tubes

Haiyang Du [a, 1], Liwu Liu [a, 1], Fenghua Zhang [b], Wei Zhao [a], Jinsong Leng [b], Yanju Liu [a, *]

[a] Department of Astronautical Science and Mechanics, Harbin Institute of Technology, Harbin 150001, People's Republic of China
[b] Center of Composite Materials and Structures, Harbin Institute of Technology, Harbin 150080, People's Republic of China

ARTICLE INFO

Article history:
Received 23 August 2016
Accepted 8 November 2016
Available online 12 November 2016

Keywords:
Shape memory tubes
Thermal-mechanical behavior
Deformation
Free-recovery and constrained recovery

ABSTRACT

Styrene-based shape memory polymer (SMP) tubes were fabricated and their basic mechanical properties in different deformation states were investigated. The tensile, compression, bending and twisting shape memory properties of the tubes were analyzed and discussed, and the results indicated that SMP tubes exhibit good shape fixity ratio and shape recovery ratio. In addition, the shape recovery behavior was investigated at different heating rates. These experimental results will provide guidance for future applications of SMP tube structures.

1. Introduction

Shape memory polymers (SMPs) are a class of stimulus-responsive materials, which retain a temporary shape and recover the original state in response to various external stimuli, such as temperature, electricity, light, solutions, etc. [1–5]. Due to the unique advantages of large deformation, widely tailored transition temperature and low cost, SMPs and their composites are attracting more and more attentions [6,7]. Nowadays, many achievements have been obtained in the synthesis technology, properties characterization, structure fabrication, experimental investigation and theory analysis. Various SMPs have been successfully synthesized, mainly including polyurethane-based SMP [8,9], styrene-based SMP [10,11], epoxy-based SMP [12–14], cyanate ester-based SMP [15,16] and polyamide-based SMP [17,18]. Moreover, various actuation methods have been developed to trigger SMPs and their composites. SMPs can be classified according to the activation method, for example temperature-induced SMP [19], electricity-induced SMP [20], light-induced SMP [21], microwave-induced SMP [22], magnetic-induced SMP [23], and water/solution-induced SMP [24], etc. Furthermore, many deformation structures have been proposed from one-way SMPs through two-way SMPs and multistage SMP to realize more complex functions [25–27]. The application fields have also covered a wide range, including aerospace engineering (hinge, truss, boom and reflector, etc.) [28–30], bio-medicine (suture, stent and orthodontics etc.) [31–33] and textile industry (coatings, finishing, weaving and knitting, etc.) [34–36]. For theoretical analysis of SMP materials, two general approaches have been used, one based on classical viscoelastic theory and the other based on phase transform theory [37–39].

Current experimental investigations are mostly focusing on SMP plates [40–42]. In contrast, there is little literature concerning the mechanical behavior of SMP tubes which are commonly used as actuators or smart deformable structures [43–48]. Baghani M et al. [43,44] built a three-dimensional SMP constitute model and simulated the shape memory effect of SMP tubes. Leng et al. [45] designed and fabricated an eight paws release device and tested the twisting recovery using electrical resistor-based heating, however they did not consider the effect of heating rate on these tubes. In addition, Yakacki et al. [46] synthesized acrylate-based SMPs that have been considered for biomedical applications. Takashima et al. [47,48] also reported the bending and rotation mechanism in SMP pneumatic actuators.

In this study, we fabricated styrene-based SMP tubes and analyzed their mechanical properties including tensile, compression, bending and twisting deformation properties. These results will provide experimental guidance for future applications. This study is organized as follows. Sections 2: the basic static and dynamic properties of SMPs were characterized by static tensile test and dynamic mechanical analysis to obtain elastic modulus and

* Corresponding author.
E-mail address: yj_liu@hit.edu.cn (Y. Liu).
[1] These authors contributed equally to this work.

http://dx.doi.org/10.1016/j.polymertesting.2016.11.011

glass transition temperature. Section 3: tensile, compression, bending and twisting experiments were designed and analyzed under different load conditions, and the shape fixity and recovery ratios were measured by free-recovery and constrained-recovery experiments, respectively. Section 4 summaries our conclusions.

2. Basic mechanical properties of SMP materials

2.1. Materials

Thermosetting styrene-based SMPs were used to fabricate SMP tubes for tensile, compression, bending and twisting experiments. The detailed synthesis and curing processes were retained by Harbin Institute of Technology (HIT), the process can be shown in Ref. [11]. Dumbbell samples were used to test the static mechanical properties based on the standard of ASTM D638. Rectangular plate samples were cut to study the dynamic mechanical properties of SMP.

2.2. Static tensile test for SMP

Tensile experiments under isothermal temperature condition were carried out from 22 °C to 82 °C with increments of 10 °C, five samples were tested at every temperature. A Zwick010 tensile machine with 1 kN load cell was used to measure the maximum load and elastic modulus at a rate of 2 mm/min until the specimens broke. The sizes of specimens were cut as 115 mm × 6 mm × 2.89 mm according to ASTM D638. The deformation-load curves at different temperatures are shown in Fig. 1.

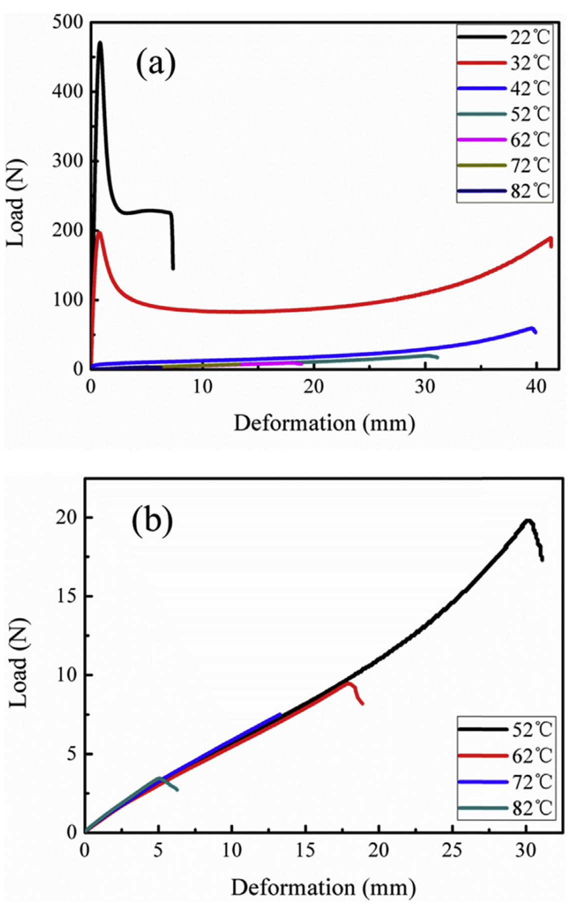

Fig. 1. Deformation-load curves at different temperatures. (a) Temperature ranges from 22 °C to 82 °C; (b) Temperature ranges from 52 °C to 82 °C.

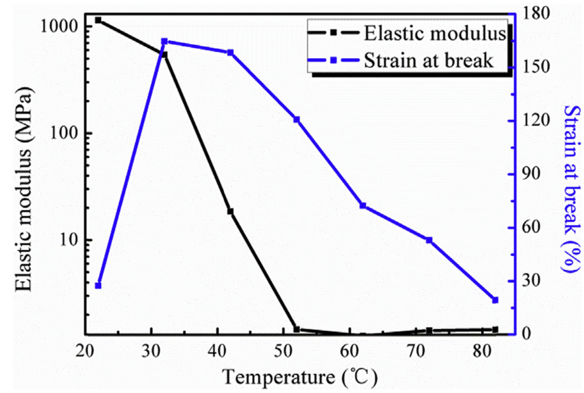

Fig. 2. Tensile properties of SMP materials at different temperatures. Elastic modulus curve from 22 °C to 82 °C (Black color); Strain at breaking point curve from 22 °C to 82 °C (Blue color). (For interpretation of the references to colour in this figure legend, the reader is referred to the web version of this article.)

Fig. 1(a) shows that the load curves begin to obviously yield when the temperature is lower than 42 °C. The maximum load declined quickly when the temperature was above 32 °C and the curves exhibited a similar trend when the temperature was above 42 °C. In order to better understand the relationship between deformation and load, the curves above 52 °C are re-plotted in Fig. 1(b). The elastic modulus and strain at the material breaking point are plotted in Fig. 2. The elastic modulus decreased quickly from 22 °C to 82 °C, SMPs gradually changed from glass state to rubber state. When the temperatures were above 52 °C, the elastic modulus was near constant which meant that the SMPs were in the rubber state. In addition, the strain at breaking point (deformation divided by gage length 25 mm) first increased and then declined with increasing temperature. The critical value was between 32 °C and 42 °C, meaning that the SMP possessed best deformation ability in this temperature range.

2.3. Dynamic mechanical analysis

Dynamic mechanical analyzer (DMA) from 01Db-Metravib (France) was used to characterize the basic dynamic mechanics (Storage modulus, loss modulus and loss factor) of SMP materials. The dimension of sample was 33.4 mm × 11.6 mm × 2.89 mm and the single/dual-cantilever mode with displacement-controlled load was applied from 25 °C to 120 °C at different heating rates. The glass transition temperatures of SMPs were obtained by three methods, including deviation peak value of storage modulus (Method 1), peak value of loss modulus (Method 2) and peak value of loss factor (Method 3) [49–51], as shown in Fig. 3. The results demonstrated the glass transition temperatures derived from peak value of loss modulus and deviation peak value of storage modulus were obviously lower than the peak value of loss factor. The transition temperature ranged from 42.65 °C to 81.27 °C at different heating rates. In our work, the low temperature (room temperature) and high temperature (80 °C) were used as critical temperature to hold temporary shape and recover the initial shapes of SMP tubes under different deformation conditions in the following section, such as investigate tensile, compression, bending and twisting deformation.

3. Shape memory experiments and analysis

3.1. Thermomechanical cycle for SMP materials

In general, a typical thermomechanical cycle has five steps. Step

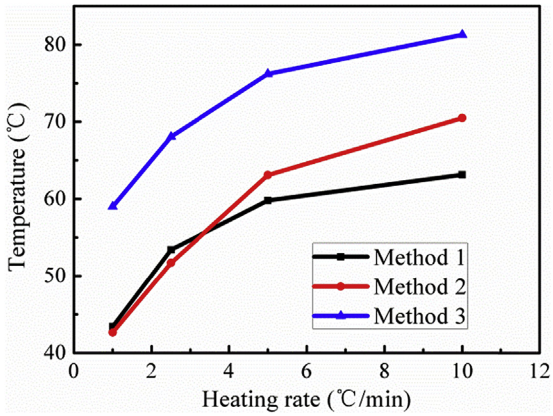

Fig. 3. Glass transition temperatures of SMP materials at different heating rates.

①: Fabricating the SMP tube and heating it above the glass transition temperature. Step ②: Holding the high temperature and deforming the SMP tube into pre-deformed shape. Step ③: Holding the pre-deformed shape and reducing the temperature below the glass transition temperature. Step ④: Holding the low temperature and removing the load. Step ⑤ includes two conditions; (i) free-recovery experiment: Maintaining a 0 N load and reheating the sample above the glass transition temperature, and (ii) constrained-recovery experiment: Maintaining the pre-deformed shape after removing the load and reheating above the glass transition temperature. The temperature-time curve and load-time curve of free-recovery and constrained-recovery experiments are shown in Fig. 4.

3.2. Free-recovery test for tensile deformation

For the free-recovery thermomechanical shape memory process, the load should be 0 N after removing the load at low temperature. In order to maintain the straight shape of the SMP tube, the load is held at a small value during the reheating process. Finally, the pre-deformed shape gradually recovers the original shape with increasing temperature.

SMP tubes with inner diameter 36 mm, outer diameter 40 mm and total length 115 mm were fabricated for the tensile

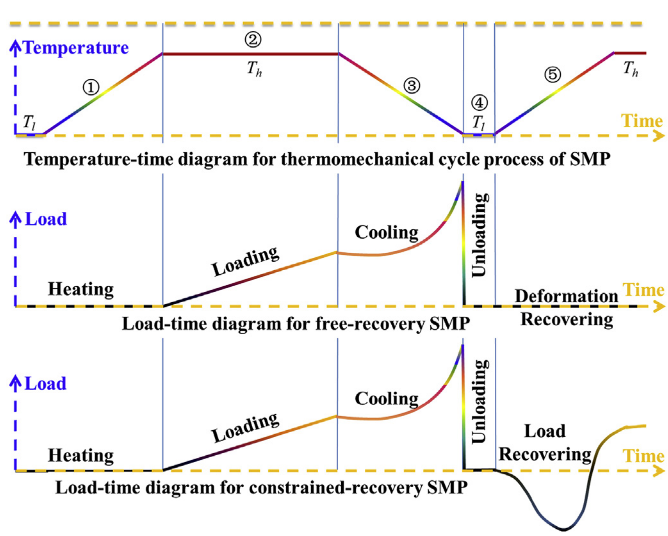

Fig. 4. Temperature-time curves and load-time curves of SMP.

experiments. The hose clamps, end fixity and load bearing devices were assembled together to form the tensile structures. A Zwick010 tensile machine equipped with a 1 kN load cell and temperature chamber was used during the deformation and recovery stages of the tensile test. As shown in Fig. 5, a small pre-load is used to keep the tubes straight. First, the sample was deformed by 5 mm at high temperature (80 °C), which amounted to a 5% strain for the SMP tube (the net distance was 100 mm between the two end hose clamps). Since the SMP tube was in the rubber state, the load was small, only about 14.5 N. Afterwards, the sample was cooled and the load was removed. After that, a small load of about 1 N was applied to keep the tube straight. Finally, the sample was reheated to recover the shape.

Fig. 6 shows the shape memory properties of SMP tubes at different heating rates. As shown in Fig. 6(a), the higher the heating rate, the more the curves move towards a higher temperature. Both the start and end temperature for shape recovery are significantly different. The start temperature increased from 42 °C at 2.5 °C/min to 55 °C at 10 °C/min, and the end temperature increased from 60 °C at 2.5 °C/min to 80 °C at 10° C/min. The heating rates had an obvious effect on the recovery process. The shape fixity ratios are higher than 97% and the shape recovery ratios are higher than 95% after the samples are reheated above the glass transition temperature, as shown in Fig. 6(b). These results verified that the SMP tubes exhibited good shape memory behavior.

It was noted that the thermal expansion effect was obvious when the temperature was low, so the deformation increased at the initial step. After that, the deformation recovered quickly to the original state. The recovery rate increased and recovery time reduced with increasing heating rate. In addition, due to limitations of the Zwick010 machine, it was difficult to record the recovery deformation at small loads (1 N), so the reported peak values of the load curves always exceeded 1 N during the heating process. The load curves at different heating rates were similar with a Gaussian function distribution, which can avoid the shock effect during the recovery process.

3.3. Constrained-recovery test for tensile deformation

For the constrained-recovery process, the deformation

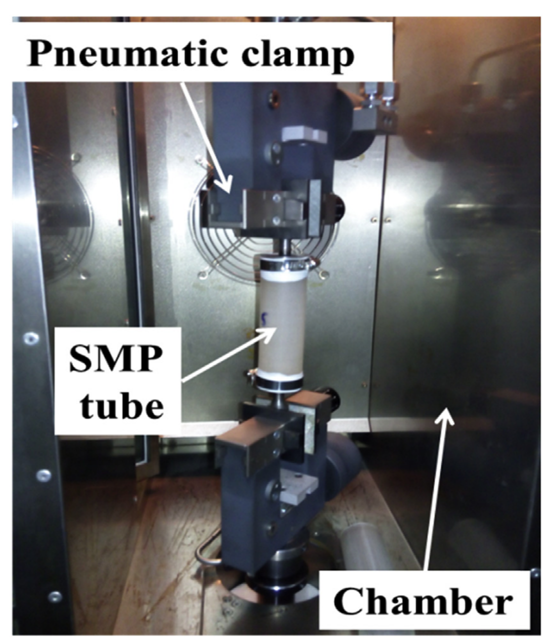

Fig. 5. Tensile test setup for the SMP tubes.

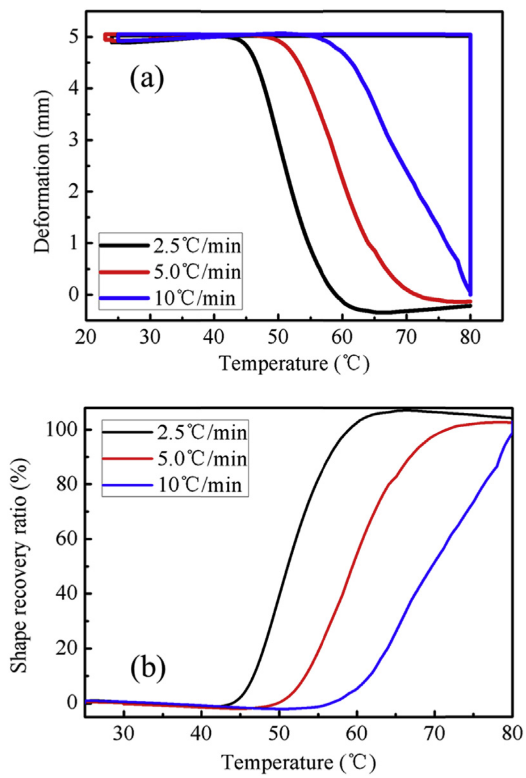

Fig. 6. Shape memory properties of SMP tubes during free-recovery test. (a)Temperature-deformation curves of SMP tubes; (b) Temperature-shape recovery ratio curves of SMP tubes.

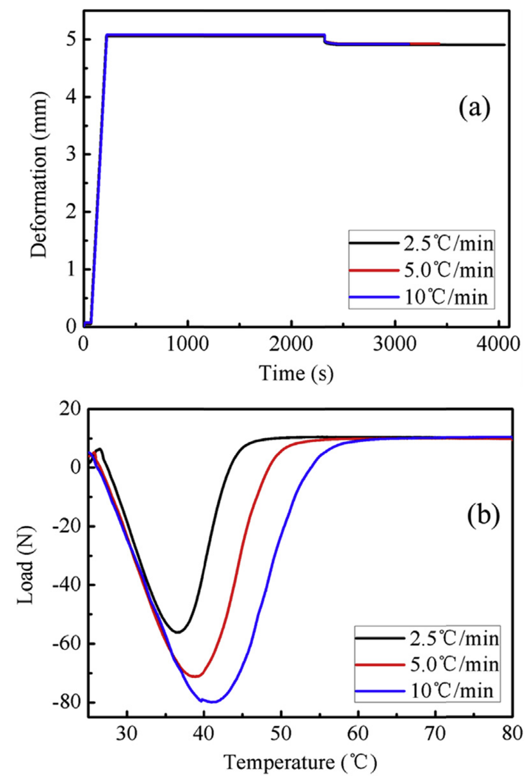

Fig. 7. Shape memory properties of SMP tubes during constrained-recovery test. (a) Time-deformation curves of SMP tubes; (b) Load recovery curves of SMP tubes.

maintained constant after removing the load at low temperature. The load changed with increasing temperature under constant deformation state during the constrained-recovery process. In our work, the original deformation at high temperature was the same as for the free-recovery test. The shape memory properties of constrained-recovery SMP tubes are shown in Fig. 7.

Fig. 7(a) shows that the deformation declined little after removing the load at low temperature. The shape fixity ratios are more than 97%. The deformation-load curves were linear for small strain deformations (<5%), and the SMP tubes can be assumed as elastic materials during the deformation process. As shown in Fig. 7(b), the load gradually comes back to the original pre-deformed values in the constrained-recovery test, and the load curves change as the temperature increases. At first, the values decreased due to the thermal expansion effect of SMP tubes. Beyond the turning point, the values gradually increase with temperature until the original shape is recovered, due to the release of stored strain during the cooling step. The compression values increased at the turning point shifted to higher temperatures with increased heating rate.

3.4. *Free-recovery test for compression deformation*

Apart from the tensile deformation, the compression behavior in the radial direction was also investigated. Such deformation and recovery properties are commonly used in biomedical application [33,46]. The main advantages include the large compressive volume ratio and the good shape recovery ability. SMP tubes identical to those used during the tensile experiments were used to analyze the radial compression properties, with an experimental setup that included PMMA plates, steel rulers and a camera, as shown in Fig. 8(a). The PMMA plates were assembled into a support structure along with, two vertical steel rulers and the camera to record temperature induced shape recovery process. The shape recovery behavior at different heating rates is plotted in Fig. 8(b). The recovery temperature increased from 40 °C at 2.5 °C/min to 55 °C at

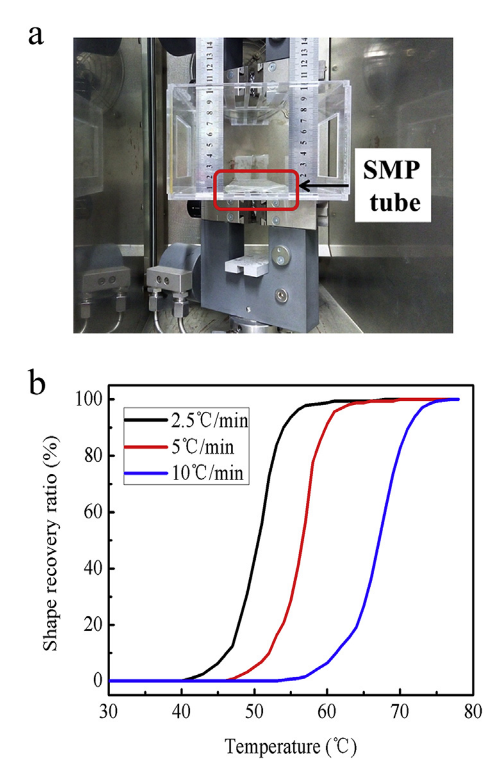

Fig. 8. (a). Experimental setup for compression test; (b). Shape recovery curves during compression test.

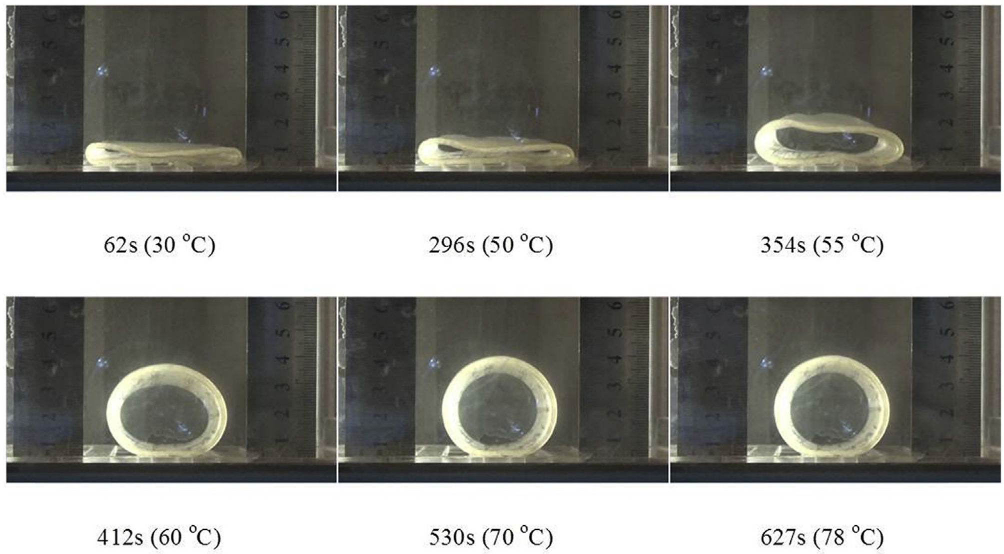

Fig. 9. Shape recovery process of compressed SMP tubes.

10 °C/min. However, the shape recovery profiles were similar and the original circular shapes were recovered at all heating rates.

Images extracted from the video record were used to characterize the shape recovery behavior at different heating rates. Fig. 9 shows the shape recovery behavior at a heating rate of 5 °C/min. Starting at 30 °C, the tube was initially in a compressed state; afterwards, with the temperature raised to 50 °C, the tube began the recovery process, with further recovery of the cross-sectional profile at 55 °C and 60 °C. With the temperature raised to 70 °C and beyond, the original shape was fully recovered and the total recovery time was 627 s from room temperature to 78 °C.

3.5. Free-recovery test for bending deformation

To investigate the potential aerospace applications such as hinges, booms and support parts of antenna [29], an experiment was set to analyze the bending behavior of SMP tubes. The experimental setup included a PMMA plate acting as a cuboid support structure, mounted inside a temperature controlled chamber with a camera to record the temporal deformation, as shown in Fig. 10(a). The shape recovery behavior at different heating rates is shown in Fig. 10(b). Although the heating rates influenced the shape recovery behavior, the tubes consistently recovered the initial shapes.

Fig. 11 shows the shape recovery behavior at a heating rate of 5 °C/min. There was very limited shape recovery as temperature up to 50 °C, but obvious recovery between 50 °C and 60 °C. At temperatures above 60 °C, the sample returned to the original straight shape.

3.6. Free-recovery test for twisting deformation

The twisting tubes can be used for aerospace applications, such as release devices [45]. The main advantages lie in the releasing of storage strain with increasing temperature. The twisting behavior of SMP tubes were investigated as a function of twisting angle. The experimental setup made of PMMA plate is shown in Fig. 12. From the top view of torsion setup, the SMP tube was twisted into the spiral shape by hand at high temperature and then the temporary shape held with decreasing temperature, the shape was different from the simulated contours of reference [43,44], in which the surface of SMP tube has not happened obviously wrinkle. A protractor was fixed on the support structure to measure the recovery

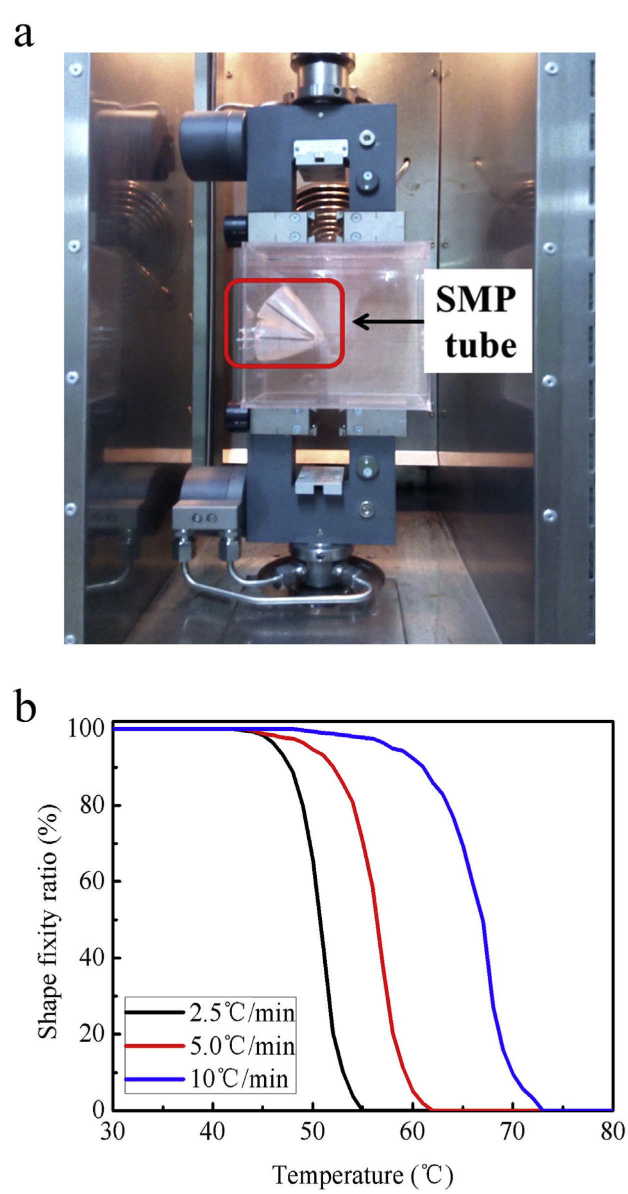

Fig. 10. (a). Experimental setup for bending test; (b). Shape recovery curves during bending test.

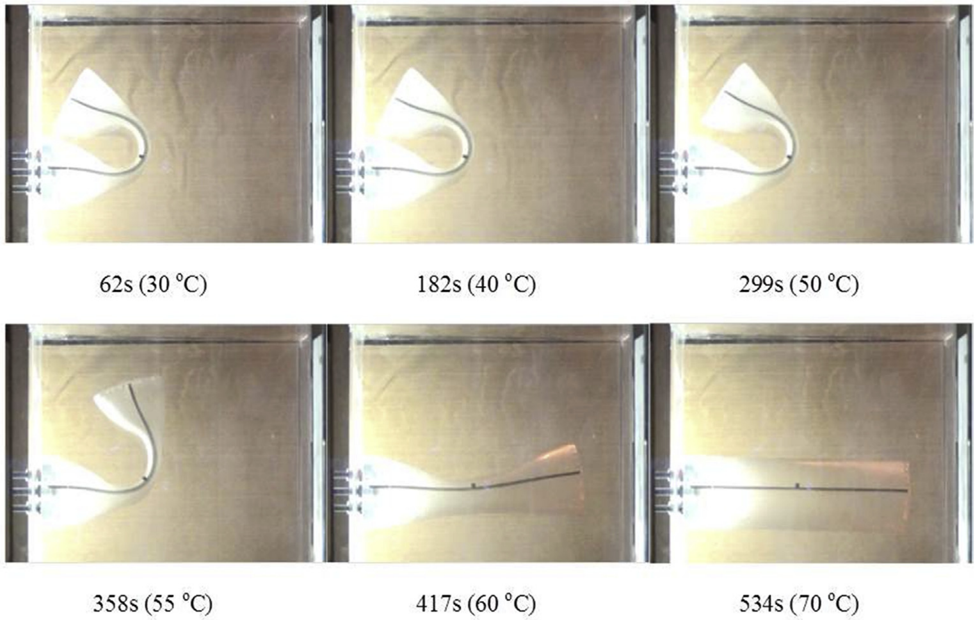

Fig. 11. Shape recovery process of bending SMP tubes.

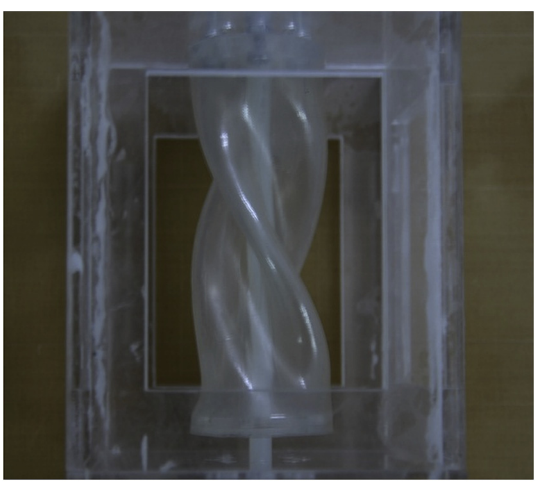

Fig. 12. Top view of experimental setup for twisting test.

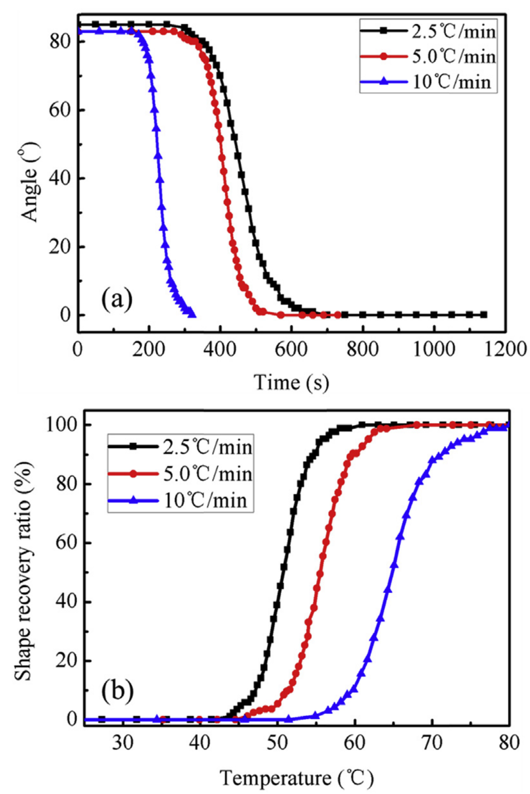

Fig. 13. Shape recovery process of SMP tubes during twisting test. (a) Time-angle curves of SMP tubes; (b) Temperature-shape recovery ratio of SMP tubes.

angle. The experiment setup was put into the thermal chamber and the twisted angle was set as 90°. The shape recovery processes at different heating rates are shown in Fig. 13.

Due to the elastic recovery after removing the external load at low temperature, the original angle of SMP tubes are 83°, 83°, 85° and the shape fixity ratio are 92.22%, 92.22% and 94.44%, respectively, as shown in Figure 13(a). The recovery time declined obviously with increasing heating rate and the values were 320 s, 730 s and 1140 s, respectively. The angle recovered 0° at different heating rates, which verified that the SMP tubes exhibited good shape recover performance. The shape recovery ratios at different heating rates are plotted in Figure 13(b). Although the total shape recovery trends were similar at different heating rates, the onset and end temperatures for shape recovery were different. The reason was that the low heating rate made the SMP tube reach thermal equilibrium in time, however, the high heating rate only heated the surface of SMP tube in a short time, the real temperature was lower than the recorded temperature. The results demonstrated that external environment changes significantly affected the shape recovery ability of SMP structures.

4. Conclusions

The mechanical deformation and shape memory properties of styrene-based SMP tubes were investigated in this study. Mechanical properties were characterized by static tensile testing and dynamic mechanical analysis. Tensile, compression, bending and twisting deformation experiments demonstrated that the shape fixity and shape recovery ratios of SMP tubes were all higher than 90%. Moreover, the shape recovery properties were affected by heating rate, with an increase in shape recovery onset temperature as the heating rate was increased. This work will provide experimental guidance for the future applications, including aerospace, automotive, robotics, and smart actuator etc.

Acknowledgments

This work is supported by the National Natural Science Foundation of China: Grant No. 11225211.

References

[1] F. Liu, M.W. Urban, Recent advances and challenges in designing stimuli-responsive polymers, Prog. Polym. Sci. 35 (1–2) (2010) 3–23.
[2] J.S. Leng, X. Lan, Y.J. Liu, S.Y. Du, Shape memory polymers and their composites: stimulus methods and applications, Prog. Mater. Sci. 56 (7) (2011) 1077–1135.
[3] Q. Zhao, H.J. Qi, T. Xie, Recent progress in shape memory polymer: new behavior, enabling materials, and mechanistic understanding, Prog. Polym. Sci. 49–50 (2015) 79–120.
[4] H. Meng, G.Q. Li, A review of stimuli-responsive shape memory polymer composites, Polymer 54 (9) (2013) 2199–2221.
[5] L. Sun, W.M. Huang, Z. Ding, Y. Zhao, C.C. Wang, H. Purnawali, C. Tang, Stimulus-responsive shape memory materials: a review, Mater. Des. 33 (2012) 577–640.
[6] H. Tobushi, H. Hara, E. Yamada, S. Hayashi, Thermomechanical properties in a thin film of shape memory polymer of polyurethane series, Smart Mater. Struct. 5 (4) (1996) 483–491.
[7] Z.G. Wei, R. Sandstrom, S. Miyazaki, Shape memory materials and hybrid composites for smart systems-Part I shape memory materials, J. Mater. Sci. 33 (15) (1998) 3743–3762.
[8] B.K. Kim, J.S. Lee, Y.M. Lee, J.H. Shin, S.H. Park, Shape memory behavior of amorphous polyurethanes, J. Macromol. Science-Physics B40 (6) (2001) 1179–1191.
[9] J.W. Cho, J.W. Kim, Y.C. Jung, N.S. Goo, Electroactive shape memory polyurethane composites incorporating carbon nanotubes, Macromol. Rapid Commun. 26 (5) (2005) 412–416.
[10] R. Beblo, K. Gross, L.M. Weiland, Mechanical and curing properties of a styrene-based shape memory polymer, J. Intelligent Material Syst. Struct. 21 (7) (2010) 677–683.
[11] D.W. Zhang, Y.J. Liu, K. Yu, J.S. Leng, Influence of cross-linking agent on thermomechanical properties and shape memory effect of styrene shape memory polymer, J. Intelligent Material Syst. Struct. 22 (18) (2011) 2147–2154.
[12] T. Xie, I.A. Rousseu, Facile tailoring of thermal transition temperatures of epoxy shape memory polymers, Polymer 50 (8) (2009) 1852–1856.
[13] J.S. Leng, X.L. Wu, Y.J. Liu, Effect of a linear monomer on the thermomechanical properties of epoxy shape memory polymer, Smart Mater. Struct. 18 (9) (2009) 095031.
[14] J.S. Leng, F. Xie, X.L. Wu, Y.J. Liu, Effect of the gamma-radiation on the properties of epoxy-based shape memory polymers, J. Intelligent Material Syst. Struct. 25 (10) (2014) 1256–1263.
[15] R. Biju, C. Gouri, C.P.R. Nair, Shape memory polymers based on cyanate ester-epoxy-poly (tetramethyleneoxide) co-reacted system, Eur. Polym. J. 48 (3) (2012) 499–511.
[16] F. Xie, L.N. Huang, Y.J. Liu, J.S. Leng, Synthesis and characterization of high temperature cyanate-based shape memory polymers with functional polybutadiene/acrylonitrile, Polymer 55 (23) (2014) 5873–5879.
[17] X.L. Xiao, D.Y. Kong, X.Y. Qiu, W.B. Zhang, F.H. Zhang, L.W. Liu, Y.J. Liu, S. Zhang, Y. Hu, J.S. Leng, Shape memory polymers with adjustable high glass transition temperatures, Macromolecules 48 (11) (2015) 3582–3589.
[18] X.L. Xiao, D.Y. Kong, X.Y. Qiu, W.B. Zhang, Y.J. Liu, S. Zhang, F.H. Zhang, Y. Hu, J.S. Leng, Shape memory polymers with high and low temperature resistant properties, Sci. Rep. 5 (2015) 14137.
[19] K. Wang, G.M. Zhu, Y.K. Wang, F. Ren, Thermal and shape memory properties of cyanate/polybutadiene epoxy/polysebacic, J. Appl. Polym. Sci. 132 (23) (2015) 42045.
[20] Y.J. Liu, H.B. Lv, X. Lan, J.S. Leng, S.Y. Du, Review of electro-active shape memory polymer composite, Compos. Sci. Technol. 69 (13) (2009) 2064–2068.
[21] H.Y. Jiang, S. Kelch, A. Lendlein, Polymers move in response to light, Adv. Mater. 18 (11) (2006) 1471–1475.
[22] F.H. Zhang, T.Y. Zhou, Y.J. Liu, J.S. Leng, Microwave synthesis and actuation of shape memory polycaprolactone foams with high speed, Sci. Rep. 5 (2015) 11152.
[23] F.H. Zhang, Z.C. Zhang, C.J. Luo, I.T. Lin, Y.J. Liu, J.S. Leng, S.K. Smoukov, Remote, fast actuation of programmable multiple shape memory composites by magnetic fields, J. Mater. Chem. C 3 (43) (2015) 11290–11293.
[24] W.M. Huang, B. Yang, L. An, C. Li, Y.S. Chan, Water-driven programmable polyurethane shape memory polymer: demonstrate and mechanism, Appl. Phys. Lett. 86 (11) (2005) 114105.
[25] S.J. Chen, J.L. Hu, H.T. Zhou, Y. Zhu, Two-way shape memory effect in polymer laminates, Mater. Lett. 62 (25) (2008) 4088–4090.
[26] M. Behl, A. Lendlein, Triple-shape polymers, J. Mater. Chem. 20 (17) (2010) 3335–3345.
[27] W.B. Li, Y.J. Liu, J.S. Leng, Shape memory polymer nanocomposite with multi-stimuli response and two-way reversible shape memory behavior, RSC Adv. 4 (106) (2014) 61847–61854.
[28] I.K. Kuder, A.F. Arrieta, W.E. Raither, P. Ermanni, Variable stiffness material and structural concepts for morphing applications, Prog. Aerosp. Sci. 63 (2013) 33–55.
[29] Y.J. Liu, H.Y. Du, L.W. Liu, J.S. Leng, Shape memory polymers and their composites in aerospace applications: a review, Smart Mater. Struct. 23 (2) (2014) 023001.
[30] X. Lan, Y.J. Liu, H.B. Lv, X.H. Wang, J.S. Leng, S.Y. Du, Fiber reinforced shape memory polymer composite and its application in a deployable hinge, Smart Mater. Struct. 18 (2) (2009) 024002.
[31] A. Lendlein, R. Langer, Biodegradable, elastic shape memory polymers for potential biomedical application, Science 296 (5573) (2002) 1673–1676.
[32] W.M. Huang, C.L. Song, Y.Q. Fu, C.C. Wang, Y. Zhao, H. Purnawali, H.B. Lv, C. Tang, Z. Ding, J.L. Zhang, Shaping tissue with shape memory materials, Adv. Drug Deliv. Rev. 65 (4) (2013) 515–535.
[33] W. Small, P. Singhal, T.S. Wilson, D.J. Maitland, Biomedical applications of thermally activated shape memory polymers, J. Mater. Chem. 20 (17) (2010) 3356–3366.
[34] J.L. Hu, S.J. Chen, A review of actively moving polymers in textile applications, J. Mater. Chem. 20 (17) (2010) 3346–3365.
[35] J.L. Hu, Y. Zhu, H.H. Huang, J. Lu, Recent advances in shape memory polymers: structures, mechanism, functionality, modeling and applications, Prog. Polym. Sci. 37 (12) (2012) 1720–1763.
[36] J.L. Hu, H.P. Meng, G.Q. Li, S.I.A. Lbekwe, Review of stimuli-responsive polymers for smart textile applications, Smart Mater. Struct. 21 (5) (2012) 053001.
[37] H. Tobushi, T. Hashimoto, S. Hayashi, E. Yamada, Thermomechanical constitutive modeling in shape memory polymer of polyurethane series, J. Intelligent Material Syst. Struct. 8 (8) (1997) 711–718.
[38] H. Tobushi, K. Okumura, S. Hayashi, N. Ito, Thermomechancial constitutive model of shape memory polymer, Mech. Mater. 33 (10) (2001) 545–554.
[39] Y.P. Liu, K. Gall, M.L. Dunn, A.R. Greenberg, J. Diani, Thermomechanics of shape memory polymers: uniaxial experiments and constitutive modeling, Int. J. Plasticity 22 (2) (2006) 279–313.
[40] J. Diani, C. Fredy, P. Gilormini, Y. Merckel, G. Regnier, I. Rousseau, A torsion test for the study of the large deformation recovery of shape memory polymers, Polym. Test. 3 (3) (2011) 335–341.
[41] J. Diani, P. Gilormini, C. Fredy, I. Rousseau, Predicting thermal shape memory polymer of crosslinked polymer networks form linear viscoelasticity, Int. J. Solid Struct. 49 (5) (2012) 793–799.
[42] R. Sujithra, S.M. Srinivasan, A. Arockiarajan, Shape recovery studies for coupled deformations in an epoxy based amorphous shape memory polymer, Polym. Test. 48 (2015) 1–6.
[43] M. Baghani, R. Naghdabadi, J. Arghavani, S. Sohrabpour, A constitutive model for shape memory polymers with applications to torsion of prismatic bars, J. Intelligent Material Syst. Struct. 23 (2) (2012) 107–116.
[44] M. Baghani, R. Naghdabadi, J. Arghavani, A semi-analytical study on helical springs made of shape memory polymer, Smart Mater. Struct. 21 (4) (2012) 045014.
[45] H.Q. Wei, L.W. Liu, Z.C. Zhang, H.Y. Du, Y.J. Liu, J.S. Leng, Design and analysis of smart release devices based on shape memory polymer composites, Compos. Struct. 133 (2015) 642–651.
[46] C.M. Yakacki, R. Shandas, C. Lanning, B. Rech, A. Eckstein, K. Gall, Unconstrained recovery characterization of shape memory polymer networks for cardiovascular applications, Biomaterials 28 (14) (2007) 2253–2263.
[47] K. Takashima, J. Rossiter, T. Mukai, McKibben artificial muscle using shape memory polymer, Sensors Actuators A- Phys. 164 (1–2) (2010) 116–124.
[48] K. Takashima, T. Noritsugu, J. Rossiter, S.J. Guo, T. Mukai, Curved type pneumatic artificial rubber muscle using shape memory polymer, J. Robotics Mechatronics 24 (3) (2012) 472–479.
[49] B. Zhou, Y.J. Liu, A glass transition model for shape memory polymer and its composite, Int. J. Mod. Phys. B 23 (6–7) (2009) 1248–1253.
[50] H.Y. DU, L.W. Liu, J.S. Leng, H.X. Peng, F. Scarpa, Y.J. Liu, Shape memory polymer S-shaped mandrel for composite air duct manufacturing, Compos. Struct. 133 (2015) 930–938.
[51] Klesa J, Placet V, Flotele E, and Collet M. Experimental evaluation of the rheological properties of Veriflex shape memory polymer, ESOMAT 2009–8th European Symposium on Martensitic Transformations, September 7–11,Czechia, 04006.